LETTERS

Toward Regional-Scale Climate Change Detection

FRANCIS W. ZWIERS

Canadian Centre for Climate Modelling and Analysis, Meteorological Service of Canada, University of Victoria, Victoria, British Columbia, Canada

XUEBIN ZHANG

Climate Monitoring and Data Interpretation Division, Meteorological Service of Canada, Downsview, Ontario, Canada

3 September 2002 and 9 October 2002

ABSTRACT

Using an optimal detection technique, the extent to which the combined effect of changes in greenhouse gases and sulfate aerosols (GS) may be detected in observed surface temperatures is assessed in six spatial domains decreasing in size from the globe to Eurasia and North America, separately. The GS signal is detected in the annual mean near-surface temperatures of the past 50 yr in all domains. It is also detected in some seasonal mean temperatures of the past 50 yr, with detection in more seasons in larger domains.

1. Introduction

A broad accumulation of evidence, including that from global-scale detection and attribution studies (see Mitchell et al. 2001 for a review), resulted in the strong conclusion in the Intergovernmental Panel on Climate Change Third Assessment Report (Houghton et al. 2001) that ''*most of the warming observed over the last 50 years is attributable to human activities.*'' However, despite the mounting evidence on the global scale, climatic change remains a rather abstract concept for local, regional, and national governments, planners, and regulators. This paper presents early evidence that the combined effect of anthropogenic greenhouse gas and sulfate aerosol forcing (GS) change over the past century is now detectable on the more relevant continental, or large trading block, scale.

2. Data and methods

We use the HadCRUTv dataset (Jones et al. 2001; available online at http://www.cru.uea.ac.uk). This dataset is based on a combination of monthly values of land near-surface air temperature anomalies and sea surface temperature anomalies relative to 1961–90 and is presented on a 5° (latitude) × 5° (longitude) grid. HadCRUTv and its predecessors have been used extensively in climate change detection studies.

Estimates of natural internal variability and the forced climate change signal required to apply the standard detection technique described below are computed from control and transient climate change simulations produced with two versions of the Canadian Centre for Climate Modelling and Analysis (CCCma) coupled global climate model [(CGCM1) Flato et al. 2000; (CGCM2) Flato and Boer 2001]. Both versions use the same atmosphere and ocean components. CGCM2 differs from CGCM1 in its treatments of ocean mixing and sea ice.

An ensemble of three transient climate change simulations for the period 1850–2100 is available for each of the models (Boer et al. 2000; Flato and Boer 2001). The models employ observed effective greenhouse gas forcing changes from 1850 to 1990, and projected changes based on the IS92a scenario from 1990 to 2100. The direct effect of sulfate aerosols is included by varying the surface albedo. The response to the prescribed GS forcing (the ''GS signal'') is estimated by averaging the six forced simulations. The use of a single GS signal assumes that the ratio of greenhouse to sulphate forcing response is correctly simulated and that natural external forcing factors have had only a relatively minor impact on the diagnostics in questions. A 1000-yr control simulation is also available for each model, and these are used to produce the required estimates of natural internal

Corresponding author address: Dr. Francis W. Zwiers, Canadian Centre for Climate Modelling and Analysis, Meteorological Service of Canada, University of Victoria, P.O. Box 1700 STN CSC, Victoria, BC V8W 2Y2, Canada.
E-mail: Francis.Zwiers@ec.gc.ca

variability. All simulated monthly mean surface temperatures are interpolated onto the same 5° × 5° grid as is used for the observations.

We search for the combined GS signal in the twentieth-century surface temperature record in six spatial domains of decreasing size: the entire globe, the Northern Hemisphere (NH), the Northern Hemisphere midlatitudes between 30° and 70°N (MidNH), MidNH land areas (EANA), and the Eurasian (EA) and North American (NA) regions, separately. Resolution is held roughly constant in relation to the domain size by aggregating 5° × 5° grid values into 30° × 40°, 15° × 40°, 10° × 40° boxes for the global, NH, and MidNH domains, respectively, and into 10° × 10° boxes for the EANA, EA, and NA domains. The number of boxes varies from 26 to 72.

We employ an independently implemented variant of the optimal detection method detailed in Allen and Stott (2002). This procedure involves regression $\mathbf{y} = \beta(\mathbf{s} - \mathbf{u}) + \mathbf{u}_0$ of the observed temperature record $\mathbf{y}$ onto the model-simulated signal pattern $\mathbf{s}$ using the total least squares method. Vector $\mathbf{u}_0$ represents natural residual variability that is not explained by the signals, and $\mathbf{u}$ represents noise in the signal pattern. The scaling factor β adjusts the signal amplitude so that the scaled signal best matches the observations. The signal is detected when the scaling factor estimate $\hat{\beta}$ is significantly greater than zero.

Separate regression analyses are performed for each of six overlapping five-decade periods (1900–49, 1910–59, . . . , 1950–99) in a manner similar to Stott et al. (2001). The data vector $\mathbf{y}$ for any particular period is constructed from the five-decade sequence of decadal averages of annual or seasonal [December–January–February (DJF), March–April–May (MAM), June–July–August (JJA) or September–October–November (SON)] mean temperature anomalies relative to the twentieth-century mean, calculated from the nonmissing years in the period. To avoid bias from systematically missing data, annual or seasonal means are treated as missing if even one month within the year or season is missing. Decadal means are computed if at least 6 of the 10 yr are present. Missing values are not filled in—we simply concatenate the available decadal means in a given five-decade period into a single extended space–time data vector. The signal vector $\mathbf{s}$ is obtained from the corresponding decades in the combined ensemble mean transient simulation and is sampled in space and time to match the availability of the observed decadal means.

The scaling factor is estimated using the total least squares method (see, e.g., Allen and Stott 2002). We assume that both the natural variability and signal noise have the same covariance structure. Its estimate, denoted $\hat{\mathbf{C}}_{N_1}$, is obtained from the model control data because the available instrumental record is not sufficiently long to provide a reliable estimate. The problem of overfitting is avoided by restricting $\mathbf{y}$ and $\mathbf{s}$ to a subspace of dimension p in which the variability of the estimated residual $\hat{\mathbf{u}}_0 = \mathbf{y} - \hat{\beta}(\mathbf{s} - \hat{\mathbf{u}})$ is consistent with model-simulated natural internal variability (Allen and Tett 1999; Stott et al. 2001). Uncertainty in $\hat{\beta}$ is expressed by means of a confidence interval that is estimated following Allen and Stott (2002). An independent covariance matrix estimate $\hat{\mathbf{C}}_{N_2}$ is used in this calculation to insure that the confidence interval is not negatively biased.

Covariance matrix estimates are computed from 1600 yr of model control simulation that has been organized into overlapping five-decade vectors, each sampled in space and time as the signal. The 1600 yr comprise the last 600 yr of the CGCM1 control simulation (the first 400 yr are discarded because of model drift) and the full 1000-yr CGCM2 control simulation. The long-term mean and linear trend (drift) is removed separately from the two long control segments at each grid point. The detrended control dataset is partitioned into two 800-yr subsets designated N_1 (containing the first 300 yr from CGCM1 and the first 500 yr from CGCM2) and N_2. These are used to compute $\hat{\mathbf{C}}_{N_1}$ and $\hat{\mathbf{C}}_{N_2}$.

The regression analysis is performed in the space spanned by the leading p empirical orthogonal functions (EOFs) of $\hat{\mathbf{C}}_{N_1}$. Guidance on the number of EOFs to retain in the calculation is obtained by conducting a residual consistency test (Allen and Tett 1999; Allen and Stott 2002). We check the robustness of our calculations and inferences by repeating the full analysis with datasets N_1 and N_2 interchanged.

3. Results

The residual consistency test statistic is displayed in Fig. 1 for annual mean temperatures for the globe. Results are similar in other regions. The model oversimulates space–time internal variability at low truncations in all domains because the model's dominant modes of variability are different from those of the observed system. It undersimulates internal variability at high truncations with more than approximately 20 EOFs. The former deficiency makes detection less effective by reducing the signal-to-noise ratio, while the latter could make results unreliable by overemphasizing time- and space scales on which the model simulates insufficient variance.

Figure 2 shows $\hat{\beta}$ and its 95% confidence interval as a function of EOF truncation for the 1950–99 EA annual mean temperatures. Detection is obtained at all but the lowest-order EOF truncations. The estimated scaling factor is less than but not significantly different from unity on the global scale (not shown). Uncertainty is greater in small domains, with the uncertainty for the globe being about half that for the EA region. This reflects the reduced space–time filtering of noise in the smaller domains.

Results based on the use of 15 EOFs for all domains, periods, and seasons are summarized in Table 1. The

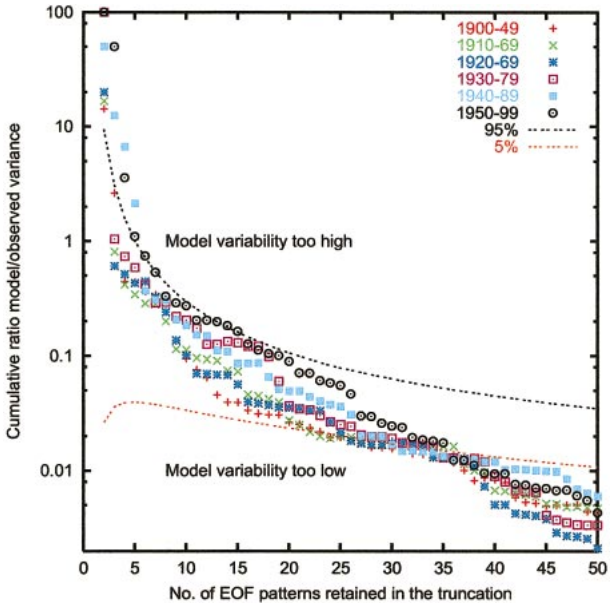

FIG. 1. Residual consistency statistic for global annual mean temperature for different 50-yr periods as a function of EOF truncation when covariance matrices $\hat{\mathbf{C}}_{N_1}$ and $\hat{\mathbf{C}}_{N_2}$ are estimated with control datasets N_1 and N_2, respectively. The dotted curves depict the 5%–95% acceptance region for the test of consistency between model-simulated and residual-observed variance. Similar results are obtained when N_1 and N_2 are interchanged.

GS signal is detected in the global domain for the periods 1900–49, 1910–59, and 1950–99. This is in agreement with results of earlier detection studies (e.g., Stott et al. 2001; Hegerl et al. 1997). The GS signal is also detected in the NH and MidNH domains for the 1900–49 and 1950–99 periods. In addition, the signal is detected in the smaller EANA, EA, and NA domains in 1950–99 and in the NA region in 1900–49.

Detection results are not very meaningful if the truncated space does not represent a substantial fraction of the untruncated signal variance $\mathbf{s}^T\mathbf{s}$. Figure 3, which displays the explained signal variance as a function of EOF truncation, shows that this is not a concern. A detection

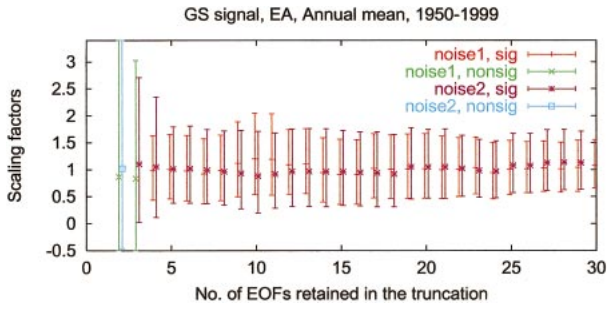

FIG. 2. Estimated GS signal scaling factors and their 95% confidence intervals for the 1950–99 EA annual mean temperatures. Noise1 (Noise2) indicates the results obtained when control dataset N_1 (N_2) is used for optimization. Sig (nonsig) indicates a scaling factor significantly (not significantly) greater than zero at the 5% level.

TABLE 1. Domains and periods in which the combined effect of greenhouse gas and direct sulfate aerosol forcing is detected at the 5% significance level in annual and/or seasonal mean surface temperatures.

Domain	1900–49	1910–59	···	1950–99
North America	Annual			Annual DJF
Eurasia				Annual DJF, MAM, SON
NH land				Annual DJF, JJA
30°–70°N	Annual DJF, JJA, SON			Annual DJF, JJA, SON
NH	Annual DJF, JJA, SON			Annual DJF, MAM, JJA
Globe	Annual DJF, MAM, SON	Annual JJA		Annual DJF, MAM, JJA

space spanned by 12 or more EOFs captures 50% or more of the signal variance in all domains. The fraction of variance explained is larger in small domains because the signal varies more coherently on the smaller time- and space scales retained in these domains.

4. Conclusions and discussion

Our finding that the effect of anthropogenic forcing is detectable in the global domain in the early and late

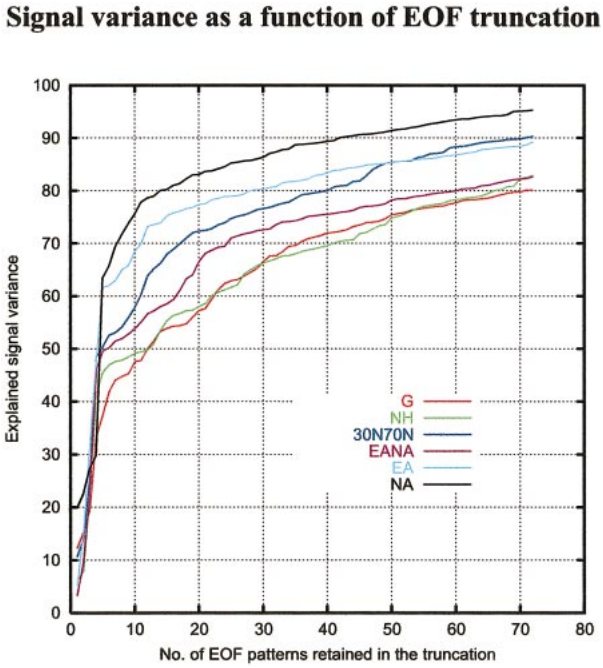

FIG. 3. Explained annual mean temperature signal variance as a function of EOF truncation averaged across the 6 five-decade periods and the two detection spaces spanned by the EOFs of control datasets N_1 and N_2.

halves of the twentieth century is in agreement with earlier detection studies. In addition, we have obtained some early evidence that the GS signal is detectable on the continental scale. In most domains, the signal scaling factor is less than, but not significantly different from, unity. The uncertainty of the scaling factor is larger in small domains because the analysis then filters out less noise from internal variability.

Corti et al. (1999) caution that the recent Northern Hemisphere warming may be more directly related to the thermal structure of a natural circulation regime that shows long-term trend, such as the Arctic Oscillation (AO; Thompson and Wallace 1998), than to anthropogenic forcing. However, Gillett et al. (2000) show that detection of a global response to changes in GS forcing is robust to the exclusion of AO-related warming. To demonstrate that our continental-scale detection results are also robust in this way, we repeated our analysis on temperature data from which the AO-related warming has been removed. To avoid uncertainty in the AO index in the early part of the century due to poor data coverage, we regressed the observed temperature data, separately for each calendar month and grid point, onto the North Atlantic Oscillation (NAO) index of Jones et al. (1997). The residuals that remain are then subjected to the analytical procedure of section 2. Detection results summarized in Table 1 continue to hold, except that the GS signal is now detected for winter mean temperature for the globe for 1910–59, but is not detected for MAM mean temperature for EA and NH for 1950–99. Thus, our detection results are generally robust to the exclusion of AO- and NAO-related warming, even on the continental scale.

We caution that the results presented here are preliminary in nature. Further investigation with other models to quantify the impact of signal uncertainty and extensions to consider multiple signals are required to increase our confidence in continental-scale detection and attribution results. Greenhouse gas, aerosol, and natural external forcing signal separation, which has not been attempted here, will be more challenging at the continental scale than at the global scale where clear delineation of the contribution from the various sources of external forcing has yet to be achieved (Mitchell et al. 2001). Nonetheless, the retention of greater signal detail at the continental scale has the potential to improve the separability of the G and S signal components because the sulfate aerosol component contains both local and remote response components. However, this will depend strongly on the fidelity of a model's regional response to forcing, and on the availability of large ensembles of forced simulations to accurately define the signals required for detection and attribution.

We anticipate that as our confidence in continental- and regional-scale detection and attribution increases, its results will have a substantial impact on the formulation of climate change policy at the national and trading block level. This will be the case for several reasons. First, simultaneously detecting a relatively detailed anthropogenic signal in multiple regions should increase the confidence of users in detection and attribution results, and thus also in model projections of future change. Second, by focusing in on continental land areas, we pose the detection and attribution question in regions where there is large natural near-surface temperature variability and where models appear to have a tendency to oversimulate that variability (Giorgi et al. 2001). Thus, concerns about the reliance on models for the estimates of internal variability required to perform detection and attribution studies should be reduced. Finally, detection and attribution at this scale demonstrates clearly to policy makers and regulators that anthropogenic changes in climate forcing are having a discernable effect in their specific area of interest. This realization should strengthen the impetus for mitigation actions that will have both local and global benefits.

Acknowledgments. We are indebted to our colleagues at CCCma who developed CGCM1 and CGCM2 and produced the long simulations used in this study. We are also appreciative of the work of Phil Jones and colleagues in the development of the HadCRUTv dataset. We thank Gabi Hegerl and Nathan Gillett for useful discussion in the course of this work; and George Boer, Greg Flato, John Fyfe, and two anonymous reviewers for comments that improved an earlier draft of this paper.

REFERENCES

Allen, M. R., and S. F. B. Tett, 1999: Checking for model consistency in optimal fingerprinting. *Climate Dyn.,* **15,** 419–434.

——, and P. A. Stott, 2002: Estimating signal amplitudes in optimal fingerprinting. Part I: Theory. *Climate Dyn.,* in press.

Boer, G. J., G. Flato, M. C. Reader, and D. Ramsden, 2000: A transit climate change simulation with greenhouse gas and aerosol forcing: Experimental design and comparsion with the instrumental record for the twentieth century. *Climate Dyn.,* **16,** 405–425.

Corti, S., F. Molteni, and T. N. Palmer, 1999: Signature of recent climate change in frequencies of natural atmospheric circulation regimes. *Nature,* **398,** 799–802.

Flato, G. M., and G. J. Boer, 2001: Warming asymmetry in climate change simulations. *Geophys. Res. Lett.,* **28,** 195–198.

——, ——, W. G. Lee, N. A. McFarlane, D. Ramsden, M. C. Reader, and A. J. Weaver, 2000: The Canadian Centre for Climate Modelling and Analysis Global Coupled Model and its climate. *Climate Dyn.,* **16,** 427–450.

Gillett, N. P., G. C. Hegerl, M. R. Allen, and P. A. Stott, 2000: Implications of changes in the Northern Hemisphere circulation for the detection of atmospheric climate change. *Geophys. Res. Lett.,* **27,** 993–996.

Giorgi, F., and Coauthors, 2001: Regional climate information—Evaluation and projections. *Climate Change 2001: The Scientific Basis, Contribution of Working Group 1 to the Third Assessment Report of the Intergovernmental Panel on Climate Change,* J. T. Houghton et al., Eds., Cambridge University Press, 583–638.

Hegerl, G. C., K. Hasselmann, U. Cubasch, J. F. B. Mitchell, E. Roeckner, R. Voss, and J. Waskewitz, 1997: Multi-fingerprint detection and attribution of greenhouse gas and aerosol forced climate change. *Climate Dyn.,* **13,** 613–634.

Houghton, J. T., Y. Ding, D. J. Griggs, M. Noguer, P. J. van der

Linden, X. Dai, K. Maskell, and C. A. Johnson, Eds.,2001: *Climate Change 2001: The Scientific Basis, Contribution of Working Group I to the Third Assessment Report of the Intergovernmental Panel on Climate Change.* Cambridge University Press, 881 pp.

Jones, P. D., T. Jonsson, and D. Wheeler, 1997: Extension to the North Atlantic Oscillation using early instrumental pressure observations from Gibraltar and South-West Iceland. *Int. J. Climatol.*, **17,** 1433–1450.

——, T. J. Osborn, K. R. Briffa, C. K. Folland, E. B. Horton, L. V. Alexander, D. E. Parker, and N. A. Rayner, 2001: Adjusting for sampling density in grid box land and ocean surface temperature time series. *J. Geophys. Res.*, **106,** 3371–3380.

Mitchell, J. F. B., D. J. Karoly, G. C. Hegerl, F. W. Zwiers, M. R. Allen, and J. Marengo, 2001: Detection of climate change and attribution of causes. *Climate Change 2001: The Scientific Basis, Contribution of Working Group I to the Third Assessment Report of the Intergovernmental Panel on Climate Change*, J. T. Houghton et al., Eds., Cambridge University Press, 695–738.

Stott, P. A., S. F. B. Tett, G. S. Jones, M. R. Allen, W. J. Ingram, and J. F. B. Mitchell, 2001: Attribution of twentieth-century temperature change to natural and anthropogenic causes. *Climate Dyn.*, **17,** 1–21.

Thompson, D. M. J., and J. M. Wallace, 1998: The Arctic Oscillation signature in the wintertime geopotential height and temperature fields. *Geophys. Res. Lett.*, **25,** 1297–1300.